Chirped-pulse direct frequency-comb spectroscopy of two-photon transitions

Akira Ozawa* and Yohei Kobayashi†

The Institute for Solid State Physics, The University of Tokyo, 5-1-5 Kashiwanoha, Kashiwa, Chiba 277-8581, Japan and CREST, Japan Science and Technology Agency, K's Gobancho, 7, Gobancho, Chiyoda-ku, Tokyo 102-0076, Japan

(Received 4 June 2012; published 23 August 2012)

The two-photon transition of ^{87}Rb ($5S_{1/2} - 4D_{3/2}$, $5S_{1/2} - 4D_{5/2}$) in a vapor cell is investigated with direct frequency-comb spectroscopy. When strong chirp is imposed on a frequency comb, it is found that the Doppler-free signal amplitude barely degrades despite a significant reduction in peak intensity. In addition, it is found that the Doppler-broadened signal is strongly dependent on the applied chirp. We present a simple model that explains this counterintuitive behavior based on the elongated spatial extent of chirped pulses. Keeping Doppler-free signals almost constant, Doppler-broadened background signals can be strongly suppressed with chirped-pulse excitations. Consequently, in the case of uniformly distributed target atoms, chirped-pulse direct frequency-comb spectroscopy can be a useful method to improve the signal-to-noise ratio in two-photon direct frequency-comb spectroscopy.

DOI: 10.1103/PhysRevA.86.022514 PACS number(s): 32.70.Jz, 32.80.Qk

I. INTRODUCTION

Direct frequency-comb spectroscopy is expected to play an important role in extending high-precision spectroscopy into wavelength regions where it is difficult to obtain a stable narrow-linewidth continuous wave (cw) laser for spectroscopy. In a single-photon transition, a longitudinal mode of a stabilized frequency comb can be scanned over the target resonance, and high-precision spectroscopy with the frequency resolution limited by the comb linewidth can be performed [1,2]. While considering two-photon excitations where either photon originates from a different longitudinal mode, there are several pairs of comb lines that can contribute to the transition. Thus, comb-resolved high-precision spectroscopy can be performed efficiently as if utilizing a cw laser with the same average power [3–5]. Typically, frequency combs can be generated from mode-locked oscillators in near-infrared to visible wavelength regions. In the time domain, a frequency comb is composed of several evenly spaced, mutually coherent short pulses, and peak intensity can be significantly higher compared with that of a cw laser with the same average power. Consequently, nonlinear frequency conversion can be efficiently driven, thus enabling the extension of frequency combs into the midinfrared to vacuum ultraviolet (VUV) region [6–8]. Therefore, direct frequency-comb spectroscopy could be a unique method for high-precision spectroscopy at such exotic wavelengths. In the nonlinear frequency-conversion process, the spectral phase of a frequency-converted comb might be distorted for various reasons; for example, in the case of a parametric process such as second-order harmonic generation (SHG) or optical parametric oscillation (OPO), material dispersion of the nonlinear medium as well as phase mismatching could introduce chirp onto the frequency-converted pulse train. For the high-harmonic generation (HHG) process often used to generate VUV frequency combs [7,8], it is known that the intensity dependence of the single-atom response introduces complicated spectral phases for high-harmonic radiation [9,10]. The process of utilizing additional amplifiers to boost the peak intensity of the mode-locked oscillator output to achieve nonlinear frequency conversion with high efficiency may also introduce additional chirp, e.g., owing to imperfect pulse compression in the chirped-pulse amplification (CPA) system or small nonlinear phase modulations inside the fiber-based power amplifier. Therefore, it is of interest and importance to investigate how chirped pulses affect direct frequency-comb spectroscopy.

In the case of single-photon direct frequency-comb spectroscopy, the effect of chirp is limited as long as the longitudinal mode is narrow enough to ignore the spectral phase variation within the single-comb mode. Because single-photon absorption is a linear process, it can be intuitively understood that the process only depends on average power, regardless of how much chirp is imposed on the pulse. However, in the case of a two-photon transition, the contribution of comb pairs no longer coherently adds up if the spectral phase is distorted. There have been several investigations regarding the effect of chirp on a two-photon transition [5,11–15]. When the target system has an intermediate state close to half the transition energy, near-resonance effects strongly influence the dipole-moment phase created by comb-mode pairs. Therefore, such two-photon transitions with near single-photon resonance states show a complicated dependency on chirp [5,11,15]. In the case of exciting a two-photon transition without a near single-photon resonance state, it has experimentally and theoretically been demonstrated that employing Fourier-limited pulses is a sufficient but not required condition to obtain the highest excitation yield [12–14]. When the pulse is chirped owing to odd-order dispersion, the antisymmetric spectral phase perturbation cancels in pairwise excitation with two comb modes. Therefore, numbers of comb pairs can still coherently add up. On the other hand, it has been demonstrated that in Doppler-free two-photon direct frequency-comb spectroscopy with picosecond pulses, the two-photon excitation yield decreases in proportion to the inverse of the pulse duration and spectral bandwidth when second-order dispersion (group delay dispersion, GDD) is introduced [12].

*ozawa@issp.u-tokyo.ac.jp
†yohei@issp.u-tokyo.ac.jp

In this paper, we investigate chirp dependency on two-photon direct frequency-comb spectroscopy with broadband femtosecond pulses. In two-photon direct frequency-comb spectroscopy with two counterpropagating beams, both Doppler-free and Doppler-broadened excitation contribute to the signal. We show that the chirp dependency of the two-photon excitation signal behaves quite differently if one collects the signal fluorescence from uniformly distributed many atoms or from a single atom: when the uniformly distributed atoms are used as a sample, as in the case of spectroscopy with the gas cell, it is found that the signal amplitudes of the Doppler-free components are quite insensitive to chirp, whereas the Doppler-broadened signals decrease in accordance with the amount of imposed chirp. This is due to temporally elongated chirped pulses that increase the effective interaction volume and compensate for the reduction of excitation yield associated with smaller peak intensity. A simple model of chirped-pulse direct frequency-comb spectroscopy is discussed, taking into account the spatial extent of the excitation region. The demonstration shows that the signal contrast given by Doppler-free signal amplitudes over Doppler-broadened signal amplitudes significantly improves when strongly chirped pulses are used for excitation. Therefore, chirped-pulse excitation could be a useful method for two-photon direct frequency-comb spectroscopy with a high signal-to-noise ratio.

II. EXPERIMENT AND RESULTS

We utilize the $5S_{1/2} - 4D_{3/2}$ and $5S_{1/2} - 4D_{5/2}$ transition of ^{87}Rb at 1033/2 nm as a model system (Fig. 1). The frequency comb for excitation is produced by a Yb-doped fiber-based master oscillator power amplifier (MOPA) system. The schematic of the setup is shown in Fig. 2. The system runs at a repetition rate of 79.9 MHz. The master oscillator is a Yb-doped fiber oscillator that is mode locked by nonlinear

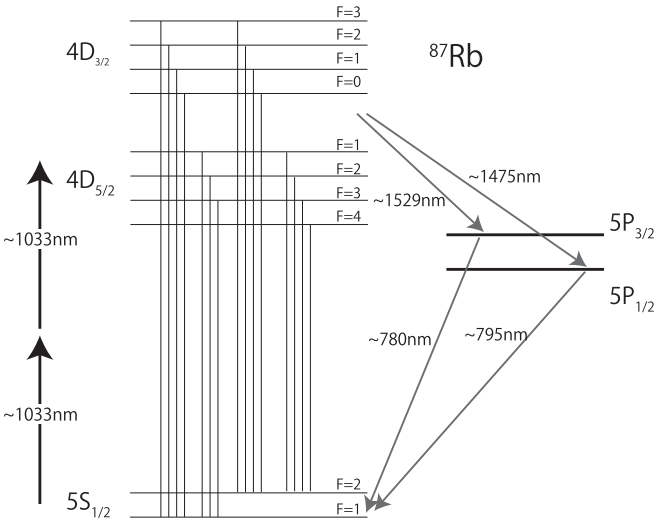

FIG. 1. Energy diagram of ^{87}Rb. $4D_{3/2}$ and $4D_{5/2}$ states are excited by two-photon absorption with frequency combs. $4D$ states decay to the ground state via $5P_{1/2}$ and $5P_{3/2}$ states. In the experiment, fluorescence at 780 nm is collected to measure the two-photon excitation yield.

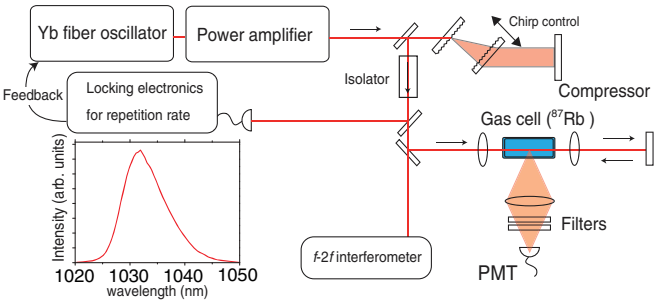

FIG. 2. (Color online) Schematic of the setup for two-photon direct frequency-comb spectroscopy of ^{87}Rb in a vapor cell. The output from the mode-locked Yb-doped fiber oscillator is amplified and sent into the gas cell filled with ^{87}Rb. The fluorescence at 780 nm is detected with a photomultiplier tube. The isolator prevents the back propagating beam from entering the power amplifier. The inset shows the laser spectrum from the power amplifier.

polarization rotation. The output from the oscillator (30 fs, 10 mW) is sent into a fiber stretcher that prolongs the pulse duration by several picoseconds. The Yb-doped fiber laser and amplifier have a gain peak at 1030 nm, which adequately matches with the required wavelength. A preamplifier boosts the weak oscillator output up to 300 mW, which is sufficient to seed the power amplifier. In the power amplifier, Yb-doped double-cladding photonic crystal fiber (DC-200-40-PZ-Yb, NKT Photonics) is pumped with 140 W of radiation from a laser diode to give up to 45 W of average output power after pulse compression. In this study, the output from the power amplifier is reduced to 4 W. A transmission grating pair (1250 lines/mm) with a total efficiency of 60% is used for compression. Pulse duration as short as ~200 fs is obtained after compression. By installing a bandpass filter after the oscillator, the output spectrum from the power amplifier is tuned to 1033 nm. The spectrum of the power amplifier output is shown in the inset of Fig. 2. Part of the amplified beam is sent to an $f - 2f$ interferometer for monitoring the carrier envelope offset frequency (f_{ceo}). The repetition frequency of the system is locked onto the rubidium rf standard with a piezoelectric transducer (PZT) actuator installed inside the oscillator. The output from the amplifier is attenuated to 190 mW and focused into the gas cell via a lens ($f = 50$ mm). The gas cell (Thorlabs) is filled with ^{87}Rb. The transmission from the gas cell is collimated with a lens ($f = 50$ mm) and reflected back into the cell after the delay line in order to excite the target with counterpropagating pulses. The delay line is adjusted such that the pulse collision point is located inside the gas cell. A very small portion of the transmission from the gas cell is detected with a slow photo diode and is used to evaluate the fluctuation of the amplifier output power that is also used to normalize the two-photon absorption signal. After excitation, the population of the $4D_{5/2}$ and $4D_{3/2}$ states decays to the ground states via the $5P_{5/2}$ and $5P_{3/2}$ states, emitting fluorescence at 1529, 1475, 780, and 795 nm (Fig. 1). The fluorescence at 780 nm is detected with a photomultiplier tube (Hamamatsu, H8259). Bandpass and notch filters are placed in front of the photomultiplier tube to block the scattered excitation beam and ambient light. A grating in the compressor is actuated by a stepper motor to continuously change the

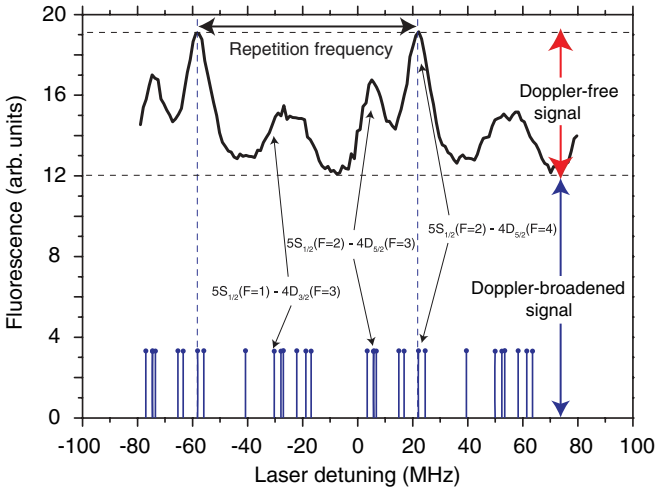

FIG. 3. (Color online) Example of the spectroscopic signal. Fluorescence intensity is plotted as a function of laser detuning at 1033/2 nm. The signal repeats itself for every repetition frequency (∼79.9 MHz). It can be seen that the fine structure of the Doppler-free signal appears on the top of broad Doppler-broadened components. Blue dots show the expected transition frequency derived from previous reports. Assignments for a few lines with major contribution are shown.

chirp imposed on the output pulse. A rather high average power (4 W) is generated from the power amplifier; however, only a small portion (190 mW) of this power is used for spectroscopy. This is to confirm that the high-power amplifier

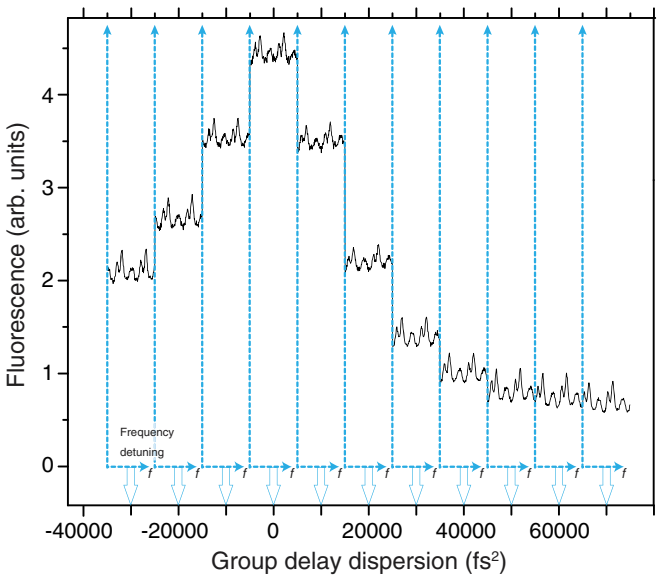

FIG. 4. (Color online) Two-photon direct frequency-comb spectroscopy of ^{87}Rb is performed with different chirp parameters imposed on excitation pulses. For each measurement, repetition frequency is swept to scan the frequency comb across resonance. The inner x axis (blue) represents frequency detuning. Measurement is repeated for different chirps imposed on the pulses (outer x axis). It can be seen that the Doppler-free signal is insensitive to the amount of chirp, whereas the Doppler-broadened signal shows a clear maximum for the chirp-free pulses.

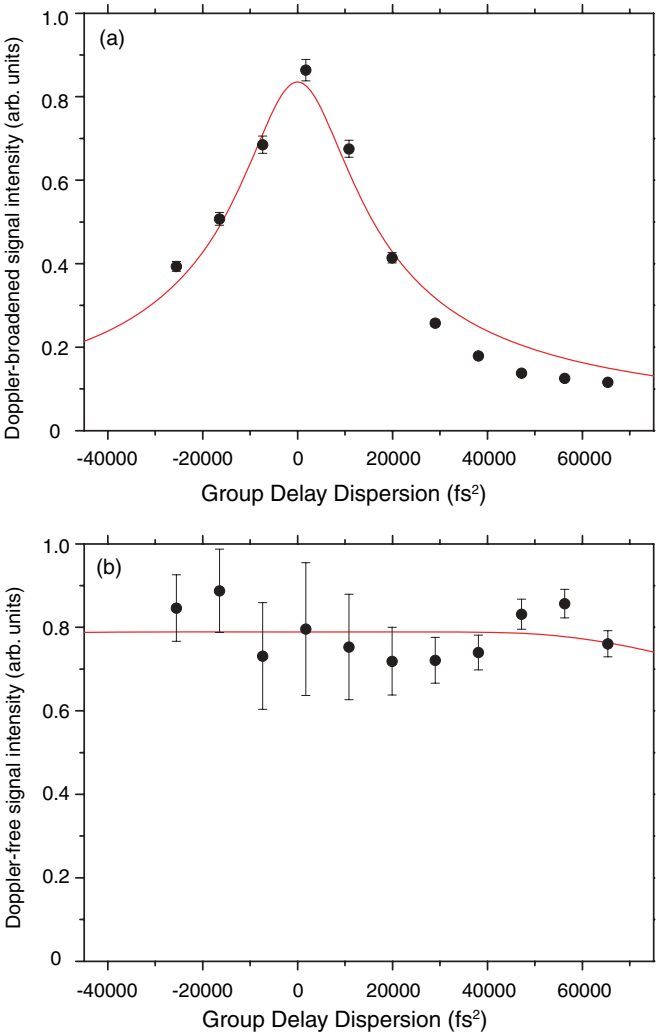

FIG. 5. (Color online) (a) Doppler-free and (b) Doppler-broadened signal amplitudes are plotted with dots as functions of the chirp applied on excitation pulses. The solid line (red) shows fitting by the model described in the text.

does not disturb the frequency-comb structure. We compared the spectroscopic signal obtained with the power amplifier output and preamplifier output and confirmed that there is no significant difference. We also tested the comb coherence of our high-power amplifier with the output power up to 10 W with another experiment [16]. For spectroscopy, the repetition rate is swept and the frequency comb is scanned across the target resonance. A typical spectroscopic signal is shown in Fig. 3. The signal repeats itself with the period of the repetition frequency. The peaklike structure that originates from the Doppler-free signal can be seen on the top of the broad background structure of the Doppler-broadened signal. The observed Doppler-free signal shows a rather complicated structure owing to the overlap of multiple lines. Although the determination of the absolute frequency is beyond the scope of this study, by utilizing the previously reported transition frequency of target transitions, we confirmed that the Doppler-free signal shape agrees with the previous report [17,18]. By changing the grating position at the pulse compressor, the measurement is repeated for different chirp parameters.

The result is summarized in Fig. 4. It can be seen that the Doppler-broadened signal is maximized with zero chirp. In contrast, the Doppler-free signal stays almost constant, independent of the applied chirp. For quantitative evaluation, the Doppler-free and Doppler-broadened signal amplitudes are extracted as a function of chirp and are shown in Fig. 5. Error bars in Fig. 5 are estimated based on the fluctuation of the signal amplitude due to amplitude noise of the driving laser.

III. DISCUSSION

A. Modeling of chirp dependency on two-photon direct frequency-comb spectroscopy

To explain the experimental finding described in the previous section, we present a model that describes the two-photon transition yield excited by the frequency comb.

The chirped electric field $E_\omega(\omega)$ for the broadband pulse with the center frequency ω_0 can be described in the angular frequency domain as follows:

$$E_\omega(\omega) = \left(4\pi\Gamma^2\frac{\Gamma^2 - iD}{\Gamma^2 + iD}\right)^{\frac{1}{4}} e^{-\frac{1}{2}(\Gamma^2 - iD)(\omega-\omega_0)^2}. \quad (1)$$

Here, a Gaussian spectral shape is assumed for the convenience of calculation. D is the amount of group delay dispersion (GDD) imposed on the pulse. Note that $\frac{\partial^2}{\partial\omega^2}\phi(\omega) = D$, where $\phi(\omega)$ represents the spectral phase. The normalization factor is defined as satisfying $\int E_\omega(\omega)E_\omega(\omega)^* d\omega = 2\pi$. Γ is inversely proportional to the FWHM of the angular frequency spectrum $\Delta\omega$,

$$\Delta\omega = 2\sqrt{\log 2}\Gamma^{-1}. \quad (2)$$

The temporal complex field $E_t(t)$ can be obtained by Fourier transforming $E_\omega(\omega)$:

$$\begin{aligned} E_t(t) &= \int E_\omega(\omega)e^{i\omega t}d\omega \\ &= \left[\frac{\Gamma^2}{\pi(\Gamma^4 + D^2)}\right]^{\frac{1}{4}} e^{-\frac{-(\Gamma^2+iD)}{2(\Gamma^4+D^2)}t^2} e^{i\omega_0 t}. \end{aligned} \quad (3)$$

The temporal complex field satisfies the normalization condition $\int E_t(t)E_t(t)^* dt = 1$. The FWHM of the temporal pulse duration $\Delta\tau$ is given by

$$\Delta\tau = 2\sqrt{\log 2}\sqrt{\frac{D^2 + \Gamma^4}{\Gamma^2}}. \quad (4)$$

For the two counterpropagating pulses along the z axis that intersect at $z = 0$, the total field $E_{\text{total}}(t)$ can be described as

$$E_{\text{total}}(t) = E_t\left(t - \frac{z}{c}\right) + E_t\left(t + \frac{z}{c}\right). \quad (5)$$

When the target two-photon transition has no near-resonance state, the excited-state amplitude (c_e) can be approximated as follows [14]:

$$\begin{aligned} c_e &\propto \int E_{\text{total}}(t)^2 e^{-i\omega_{ge}t} dt \\ &= \int \left[E_t\left(t - \frac{z}{c}\right) + E_t\left(t + \frac{z}{c}\right)\right]^2 e^{-i\omega_{ge}t} dt \\ &= c_e^+ + c_e^- + 2c_e^\pm, \end{aligned} \quad (6)$$

with

$$c_e^+(z) = \int E_t\left(t + \frac{z}{c}\right)^2 e^{-i\omega_{ge}t} dt, \quad (7)$$

$$c_e^-(z) = \int E_t\left(t - \frac{z}{c}\right)^2 e^{-i\omega_{ge}t} dt, \quad (8)$$

$$c_e^\pm(z) = \int E_t\left(t + \frac{z}{c}\right) E_t\left(t - \frac{z}{c}\right) e^{-i\omega_{ge}t} dt, \quad (9)$$

where ω_{ge} is the transition frequency. $c_e^+(z)$ [$c_e^-(z)$] are proportional to the probability amplitude where two photons are taken from a single beam propagating in the positive [negative] z direction (collinear excitation). When a single beam is responsible for spectroscopy, atoms with several velocity classes contribute to the signal, and therefore a Doppler-broadened spectrum is observed. On the other hand, $c_e^\pm(z)$ represents the two-photon excitation process at position z where a single photon is, respectively, taken from two counterpropagating beams (anticollinear excitation). In the anticollinear excitation, Doppler shift for right-going and left-going beams is canceled and thus a Doppler-free spectrum can be expected. Therefore, $|c_e^+(z)|^2 = |c_e^-(z)|^2$ represents the Doppler-broadened signal intensity, whereas the Doppler-free signal intensity is given by $|c_e^\pm(z)|^2$ at position z.

Here we investigate the case where the spectral center ω_0 is tuned to half the transition frequency ω_{ge},

$$2\omega_0 = \omega_{ge}. \quad (10)$$

By utilizing Eqs. (3) and (7)–(9), we obtain

$$|c_e^+(z)|^2 = |c_e^-(z)|^2 = \frac{\Gamma^2}{\sqrt{\Gamma^4 + D^2}}, \quad (11)$$

$$|c_e^\pm(z)|^2 = \frac{\Gamma^2}{\sqrt{\Gamma^4 + D^2}} e^{-\frac{2\Gamma^2}{D^2+\Gamma^4}(\frac{z}{c})^2}. \quad (12)$$

It is instructive to rewrite Eqs. (11) and (12) as

$$|c_e^+(z)|^2 = |c_e^-(z)|^2 \propto \frac{1}{\Delta\omega\Delta\tau}, \quad (13)$$

$$|c_e^\pm(z)|^2 \propto \frac{1}{\Delta\omega\Delta\tau} e^{-8\log 2(\frac{z}{c\Delta\tau})^2}. \quad (14)$$

Equation (14) reproduces the excited-state amplitude derived in a previous study [12]. When we limit ourselves to a small spatial region at $z = 0$, both Doppler-broadened and Doppler-free components should show the same dependency on chirp and the two-photon signal would decrease in proportional to the inverse of $\Delta\omega\Delta\tau$:

$$|c_e^+(z=0)|^2 = |c_e^-(z=0)|^2 = |c_e^\pm(z=0)|^2 \propto (\Delta\omega\Delta\tau)^{-1}. \quad (15)$$

The assumption of $z = 0$ corresponds to the experiments with a very small interaction region, such as spectroscopy on a single atom in an ion trap. In that case, the chirped pulse would decrease the two-photon excitation signal in accordance with Eq. (15), and one would try to use temporally compressed pulses to obtain high signal intensity. However, when the target atoms are spatially distributed along the beam axis, which is often the case in measurements with a vapor cell, the spatial variation (z dependency) of the probability amplitude has to be considered. It can be seen

from Eq. (14) that the spatial variation (z dependency) of the probability amplitude is related to the spatial extent of excitation pulses determined by the temporal pulse duration ($\Delta\tau$). To incorporate this spatial effect, excitation probability is integrated along the z axis to obtain two-photon signal intensity for the Doppler-broadened $|C_e|^2$ and Doppler-free $|C_e^{\pm}|^2$ components that can be compared with our experimental measurements,

$$|C_e|^2 = \int_{-\frac{L}{2}}^{\frac{L}{2}} |c_e^{+}(z)|^2 dz, \tag{16}$$

$$|C_e^{\pm}|^2 = \int_{-\frac{L}{2}}^{\frac{L}{2}} |c_e^{\pm}(z)|^2 dz. \tag{17}$$

L defines the spatial region along the z axis from which fluorescence is collected. Here we neglected the spatial variation of the field intensity along the z axis due to focusing and assumed that the excitation beams are cylindrical. Instead, we consider that the Rayleigh length of the excitation beams also limits the interaction region. In our case, fluorescence is obtained from a region much larger than the Rayleigh length of the beams. Therefore, L is set to be about the Rayleigh length of the excitation beams ($\sim$400 μm). $|C_e|^2$ and $|C_e^{\pm}|^2$ are numerically evaluated and shown as solid lines in Fig. 5. The model adequately reproduces the chirp dependency of the Doppler-broadened components. In addition, the model describes that the Doppler-free components are quite insensitive to chirp. The small systematic deviation from the model curve could be because of the contribution of the higher-order dispersions and/or tiny misalignment of the setup when the compressor grating is moved.

Under the assumption of a cylindrical beam with uniform target density, it is interesting to note that when L is taken to be infinity, $|C_e^{\pm}|^2$ can be calculated analytically and is totally independent of the amount of GDD:

$$|C_e^{\pm}|^2 = \int_{-\infty}^{\infty} |c_e^{\pm}(z)|^2 dz = c\sqrt{\frac{\pi}{2}}\Gamma. \tag{18}$$

B. Physical interpretation of the results

Here we present an intuitive argument on the chirp dependency of the two-photon direct frequency-comb spectroscopy. Because the difference between the chirp dependency of Doppler-broadened (collinear) and Doppler-free (anticollinear) excitation appears to be z dependency on the $e^{-\frac{2\Gamma^2}{D^2+\Gamma^4}(\frac{z}{c})^2}$ term in Eq. (12), we focus on the spatial extent of the excitation pulses. Figure 6(a) illustrates chirped (top) and Fourier-limited (bottom) pulses in the collinear excitation geometry. Both pulses interact with the same number of atoms distributed along the z axis. When the pulse is chirped, its peak intensity decreases and the two-photon excitation yield also decreases. Therefore, in the case of collinear excitation, the chirped pulse results in a weaker spectroscopy signal. Figure 6(b) shows two counterpropagating pulses for Doppler-free excitation when two counterpropagating pulses exactly overlap ($t = 0$). When the pulse is Fourier limited [Fig. 6(b), bottom], the interaction region is limited by the spatial length where two pulses overlap. Thus, for Fourier-limited pulses, anticollinear excitation addresses atoms inside the region defined by the pulse duration. In the case of chirped pulses, the instantaneous frequency linearly changes along the z axis. The slope of instantaneous frequency change as a function of z has opposite signs for right-going and left-going pulses [see Fig. 6(c)]. Thus, the sum of those two frequencies is independent of z and matches with the transition frequency at $t = 0$ when Eq. (10) is satisfied. Atoms may interact with two photons whose energy sum equals the transition frequency, independent of where the atom is located along the z axis. Thereby, the

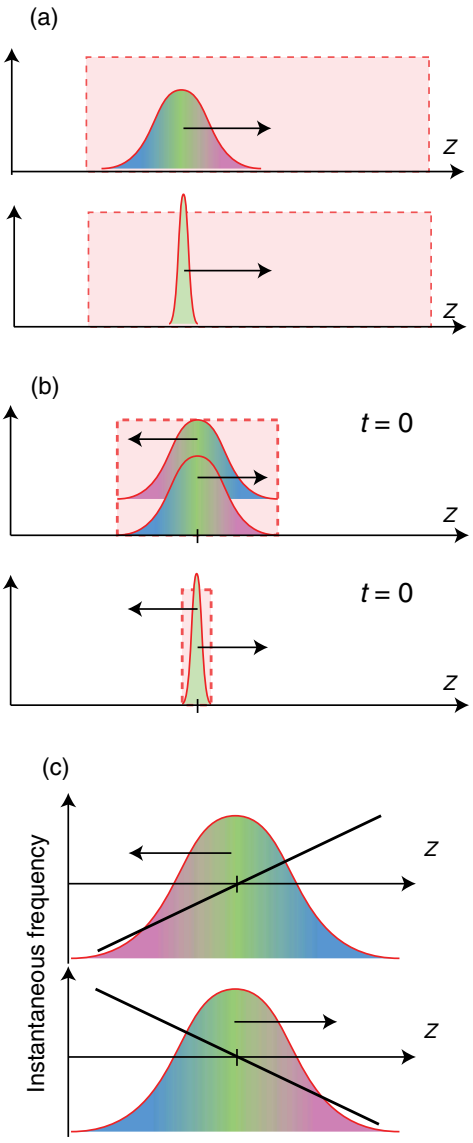

FIG. 6. (Color online) (a) Chirped (top) and Fourier-limited (bottom) pulses for collinear excitation geometry. Both chirped and Fourier-limited pulses access the same number of target atoms that distribute uniformly along the z axis (pink box). Because the chirped pulse has lower peak intensity, the two-photon yield decreases in accordance with the amount of chirp for collinear excitation. (b) Chirped (top) and Fourier-limited (bottom) pulses for anticollinear excitation geometry. Chirped pulses can address a larger interaction region (pink box) compared with Fourier-limited pulses. (c) Instantaneous frequency of two counterpropagating chirped pulses (black line). Two pulses propagating in opposite directions have frequency slopes with opposite signs.

interaction region for counterpropagating chirped pulses as well as Fourier-limited pulses is defined by the temporal pulse duration. When the pulse is chirped and the temporal pulse width increases, the number of atoms that are inside the interaction region increases accordingly. A reduction in the two-photon excitation yield due to the lower peak intensity of the chirped pulse is partially canceled by an increase in the number of target atoms inside the interaction region. Consequently, the Doppler-free anticollinear excitation of two-photon transition has weaker chirp dependency compared with that of Doppler-broadened collinear excitation. Since this effect originates from the elongated pulse duration with chirp, it is expected to be more notable for shorter and more broadband pulses where the pulse duration can be affected more strongly with GDD. Therefore, a theoretical model without considering z dependency adequately describes the excitation with chirped picosecond pulses where an increase in pulse duration is not significant [12]. This study demonstrates that the spatial position dependency of the excitation yield along a propagation axis is not negligible when chirped femtosecond pulses are used for direct frequency-comb spectroscopy.

IV. CONCLUSIONS

We investigated chirp dependency on the two-photon excitation probability in direct frequency-comb spectroscopy with broadband femtosecond pulses when the uniformly distributed ^{87}Rb atoms inside a vapor cell are used as a test target. The spectroscopy signal consists of Doppler-free components originating from anticollinear excitation and Doppler-broadened signals originating from excitation in a collinear geometry. In accordance with the imposed chirp, the peak intensity of the excitation beam decreases and the signal amplitudes of the Doppler-broadened components deteriorate as well. However, in the case of Doppler-free signals, the increased temporal duration of chirped pulses enables accessing a larger number of target atoms. Consequently, Doppler-free signals exhibit a weak dependency on chirp. This behavior is quite different from the two-photon direct frequency-comb spectroscopy with a very small interaction region, such as single-atom spectroscopy in an ion trap where a two-photon excitation signal simply decreases with the amount of applied chirp.

When nonlinear frequency conversion is employed to generate frequency combs in exotic wavelengths such as midinfrared or VUV regions, it is sometimes difficult to precisely chirp compensate the frequency-converted pulse train. When two-photon direct frequency-comb spectroscopy is to be performed with such a frequency-converted comb, our results suggest that the remaining GDD may not weaken the spectroscopy signal.

In addition, chirped-pulse two-photon direct frequency-comb spectroscopy is useful to improve its signal-to-noise ratios. In two-photon direct frequency-comb spectroscopy, a Doppler-free spectral structure that is often under investigation is on the top of the unwanted Doppler-broadened background signal. When the signal amplitude fluctuates, e.g., due to the amplitude noise of the driving laser, the Doppler-free signal is affected by the fluctuation of the Doppler-broadened signal. With strong chirp imposed on the driving pulses, the Doppler-free signals weigh more than the Fourier-limited pulses. Therefore, chirped-pulse two-photon direct frequency-comb spectroscopy can detect Doppler-free signals with better signal-to-noise ratios suppressing the Doppler-broadened components.

ACKNOWLEDGMENT

This research is supported by the Photon Frontier Network Program of MEXT, Japan.

[1] V. Gerginov, C. E. Tanner, S. A. Diddams, A. Bartels, and L. Hollberg, Opt. Lett. **30**, 1734 (2005).
[2] D. C. Heinecke, A. Bartels, T. M. Fortier, D. A. Braje, L. Hollberg, and S. A. Diddams, Phys. Rev. A **80**, 053806 (2009).
[3] Y. Baklanov and V. Chebotayev, Appl. Phys. **12**, 97 (1977).
[4] R. Teets, J. Eckstein, and T. W. Hänsch, Phys. Rev. Lett. **38**, 760 (1977).
[5] D. Felinto and C. E. E. López, Phys. Rev. A **80**, 013419 (2009).
[6] N. Leindecker, A. Marandi, R. L. Byer, and K. L. Vodopyanov, Opt. Express **19**, 6296 (2011).
[7] Ch. Gohle, Th. Udem, M. Herrmann, J. Rauschenberger, R. Holzwarth, H. Schuessler, F. Krausz, and T. W. Hänsch, Nature (London) **436**, 234 (2005).
[8] R. J. Jones, K. D. Moll, M. J. Thorpe, and J. Ye, Phys. Rev. Lett. **94**, 193201 (2005).
[9] J. Mauritsson, P. Johnsson, R. López-Martens, K. Varjú, W. Kornelis, J. Biegert, U. Keller, M. B. Gaarde, K. J. Schafer, and A. L'Huillier, Phys. Rev. A **70**, 021801 (2004).
[10] M. Lewenstein, P. Salières, and A. L'Huillier, Phys. Rev. A **52**, 4747 (1995).
[11] N. Dudovich, B. Dayan, S. M. Gallagher Faeder, and Y. Silberberg, Phys. Rev. Lett. **86**, 47 (2001).
[12] S. Reinhardt, E. Peters, T. W. Hänsch, and Th. Udem, Phys. Rev. A **81**, 033427 (2010).
[13] D. Meshulach and Y. Silberberg, Nature (London) **396**, 239 (1998).
[14] D. Meshulach and Y. Silberberg, Phys. Rev. A **60**, 1287 (1999).
[15] M. C. Stowe, F. C. Cruz, A. Marian, and J. Ye, Phys. Rev. Lett. **96**, 153001 (2006).
[16] A. Ozawa and Y. Kobayashi, in *Conference on Lasers and Electro-Optics*, Paper No. CTh5D.9 (Optical Society of America, Washington D.C., 2012).
[17] W.-K. Lee, H. S. Moon, and H. S Suh, Opt. Lett. **32**, 2810 (2007).
[18] H. S. Moon, W.-K. Lee, and H. S. Suh, Phys. Rev. A **79**, 062503 (2009).